Mechanical Systems and Signal Processing (2003) **17**(3), 683–704
doi:10.1006/mssp.2001.1463

DETERMINATION OF UNKNOWN IMPACT FORCE ACTING ON A SIMPLY SUPPORTED BEAM

BOR-TSUEN WANG AND CHUN-HSIEN CHIU

Department of Mechanical Engineering, National Pingtung University of Science and Technology, Pingtung, Taiwan 91207, Republic of China. E-mail: wangbt@mail.npust.edu.tw

(Received 20 April 2000, accepted 18 October 2001)

This work presents a predictive model for determining the location and amplitude of an unknown impact force acting on a simply supported beam. Both time and frequency domain prediction methods are developed, respectively. The structural modal parameters can be first obtained by theoretical modal analysis (TMA) or by experimental modal analysis (EMA). The structural response at time and frequency domains due to an unknown impact force can then be measured and recorded. The predicted response can also be formulated and expressed as functions of amplitude and location of the impact force. The sum of square errors between the predicted and measured response is then defined as the objective function, while the amplitude and the location of the unknown impact force are defined as design variables. The optimisation problem is thereby constructed and can be solved for the amplitude of the impact force. The mode shape information associated to the location of the impact force can also be resolved and compared to the structural mode shapes to determine the location of the unknown impact force. Both numerical and experimental prediction results are presented. Results show that the predictive model is feasible and leads to the prediction of magnitude and location of the unknown impact force for arbitrary structures as well.

1. INTRODUCTION

Force prediction is one of the inverse engineering problems [1]. Many researchers have dedicated to identify the force content acting on structures. Han and Wicks [2] applied the singular value decomposition (SVD) technique to obtain the inversion of system matrix or frequency response function (FRF) matrix, and so forth the force spectrum can be determined. Three types of measurements, including translational, rotational and curvature data, were numerically simulated to show the effectiveness of force estimation. Inoue *et al.* [3] adopted a similar approach to estimate the magnitude and direction of impact force by employing three axial force components. The impact force identification was demonstrated for a simply supported beam, when strain response was measured by strain gauges. Lim and Pilkey [4] presumed that the force location is known. With the adoption of modal reduction technique, the finite degree of freedom (dof) system matrix can be obtained. The pseudo-inverse solution is then employed instead of dynamic programming solution [5] for computational efficiency. The time history of point force acting on a 10-bay truss was well predicted. Zhu and Lu [6] presented a time domain method to identify both concentrated and distributed loads on beam and plate structures. Both the time history and the spatial distributions of the loads can be generally determined under the assumption of known load location.

It is useful for structural design and failure evaluation to know the force information. In particular, for composite laminates subject to impact, the invisible impact damage may

0888 3270/03/ + $30.00/0

occur inside structures. The prediction of impact force on composite is of interest practically. Wu *et al.* [7] developed a method to predict the time history of the impact force exerted on a laminate plate with the use of the measured strain response. The force location is also presumed to be known. They concluded that multiple strain gauges could obtain an overall better prediction of the impact force. Chang and Sun [8] also determined the transverse impact force on a composite laminate. They used experimentally generated Green's functions and performed the deconvolution of the impact response in time domain to recover the impact force time history. Although the theoretical formulation of Green function is not used, the impact force location must be known in advance.

Hollandsworth and Busby [9] studied the impact force identification for a cantilever beam structure. They stated the force identification problem as follows. 'Given the response of a structure, what impact force is required to produce?' They found that the accelerometer located close to the location of the impact force would provide better prediction of the force time history. Odeen and Lundberg [10] presented an impulse response method to predict the time history of impact force. The structural impulse response function must be determined first and thus the method implies the known force location. Liu *et al.* [11] used the non-contact sensor, laser Doppler transient anemometer (LDTA), to measure the system response for the force detection in the inverse analysis.

Among the above discussions, the impact force time history can be predicted satisfactorily for the adoption of different prediction models and different sensors. The prediction of impact force location is difficult. There is little literature dealing with the location prediction. Wu and Yeh [12] intended to identify the impact force location by comparing the reconstructed strain response among several candidate locations. Their method cannot be practically used. Doyle and his coworkers presented several papers [13–15] about force location determination. The basic scheme is based on the pattern match for the reconstructed force history. The solution of both the time history and location of impact forces are treated separately. Excessive computational effort will be required to solve the problem. Choi and Chang [16] introduced distributed piezoelectric sensors to detect the impact force time history and its location by comparing measured and estimated sensor outputs. Two loops are involved in the fitting process. One is for predicting the force time history, and the other is for predicting the force location.

The basic idea of the force identification problem is to determine the system input via the knowledge of system output. The schematics of the force prediction problem can be shown in Fig. 1. This work will develop both the time and frequency domain methods for predicting the magnitude and location of the impact force exerted on a simply supported beam. The impact force is modelled as an ideal impulse delta function. The system modal parameters can be obtained from theoretical modal analysis (TMA) or experimental

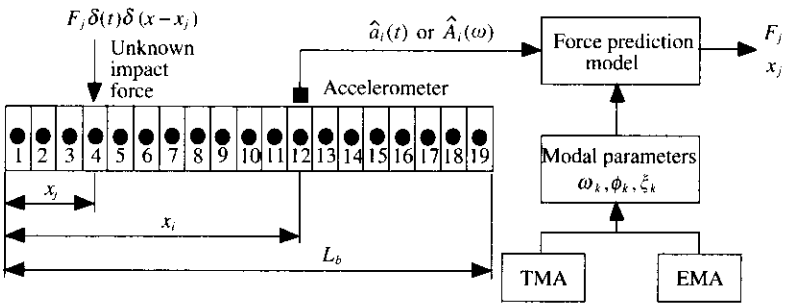

Figure 1. Schematics of impact force prediction for a simply supported beam.

modal analysis (EMA). When the accelerometer is applied to acquire the beam response, the predictive model can determine the impact force magnitude and location simultaneously.

The paper first derives the theoretical acceleration response due to the impact force in time and frequency domains. Formulation of the force predictive model is to define the optimisation problem, that the objective is to solve for magnitude and mode shape components associated with the force location, so as to minimise the errors between the predicted and measured response. By the adoption of modal assurance criterion (MAC), the location of the impact force can be predicted. Results show that the predictive model is feasible and applicable to other structures as well.

2. IMPACT FORCE RESPONSE FOR SIMPLY SUPPORTED BEAM

Consider a uniform simply supported beam as shown in Fig. 1 with the length L_b, cross-sectional area A_b, and area moment of inertia I_b, and assume an ideal impact force acting at $x = x_j$. For Euler–Bernoulli beam, the equation of motion can be shown as [17]

$$E_b I_b \frac{\partial^4 w(x,t)}{\partial x^4} + \frac{\partial}{\partial t} C_b[w(x,t)] + \rho_b A_b \frac{\partial^2 w(x,t)}{\partial t^2} = F_j \delta(t)\delta(x - x_j) \tag{1}$$

where E_b, C_b and ρ_b are the Young's Modulus, damping coefficient and density of the beam, respectively. The boundary conditions at $x = 0$ and L_b can be shown as

$$w(x = 0, t) = 0, \quad \left.\frac{\partial^2 w(x,t)}{\partial x^2}\right|_{x=0} = 0 \tag{2}$$

$$w(x = L_b, t) = 0, \quad \left.\frac{\partial^2 w(x,t)}{\partial x^2}\right|_{x=L_b} = 0. \tag{3}$$

2.1. MODAL ANALYSIS

By neglecting the damping and force terms, the system equation can be simplified as follows:

$$E_b I_b \frac{\partial^4 w(x,t)}{\partial x^4} + \rho_b A_b \frac{\partial^2 w(x,t)}{\partial t^2} = 0. \tag{4}$$

By the method of separation of variables, the system displacement response can be assumed as

$$w(x,t) = \phi(x)q(t). \tag{5}$$

By solving the eigenvalue problem, the eigenvalue can be obtained as

$$\alpha_k = \frac{k\pi}{L_b}, \quad k = 1, 2, \ldots \tag{6}$$

and so forth the system natural frequency can be expressed as follows:

$$\omega_k = \alpha_k^2 \sqrt{\frac{E_b I_b}{\rho_b A_b}} = (k\pi)^2 \sqrt{\frac{E_b I_b}{\rho_b A_b L_b^4}} \tag{7}$$

so the mode shape function is

$$\phi_k(x) = Y_k \sin \alpha_k x = \sqrt{\frac{2}{\rho_b A_b L_b}} \sin \alpha_k x \tag{8}$$

where Y_k is some constant. In particular, $Y_k = \sqrt{2/\rho_b A_b L_b}$, the following orthonormal relations can be obtained:

$$\int_0^{L_b} \rho_b A_b \phi_k(x) \phi_l(x)\, \mathrm{d}x = \delta_{kl} \tag{9}$$

$$\int_0^{L_b} E_b I_b \phi_k(x) \frac{\mathrm{d}^4 \phi_l(x)}{\mathrm{d}x^4}\, \mathrm{d}x = \omega_k^2 \delta_{kl} \tag{10}$$

$$\int_0^{L_b} C_b \phi_k(x) \phi_l(x)\, \mathrm{d}x = 2\xi_k \omega_k \delta_{kl}. \tag{11}$$

It is noted that the proportional damping is assumed, and the damping coefficient holds the relations

$$C_b = a_1 \left(E_b I_b \frac{\mathrm{d}^4 \phi_k(x)}{\mathrm{d}x^4} \right) + a_2 (\rho_b A_b) \tag{12}$$

where a_1 and a_2 are some constants.

2.2. TRANSIENT RESPONSE ANALYSIS

From expansion theorem, the beam displacement response can be assumed as

$$w(x, t) = \sum_{k=1}^{\infty} \phi_k(x) q_k(t). \tag{13}$$

By substitution of the above equation into equation (1), the multiplication of $\phi_l(x)$ and the integration over the beam length, one can obtain

$$\begin{aligned} &\sum_{k=1}^{\infty} \left(\int_0^{L_b} \rho_b A_b \phi_l(x) \phi_k(x)\, \mathrm{d}x \right) \ddot{q}_k(t) + \sum_{k=1}^{\infty} \left(\int_0^{L_b} C \phi_l(x) \phi_k(x)\, \mathrm{d}x \right) \dot{q}_k(t) \\ &\quad + \sum_{k=1}^{\infty} \left(\int_0^{L_b} E_b I_b \phi_l(x) \frac{\mathrm{d}^4 \phi_k(x)}{\mathrm{d}x^4}\, \mathrm{d}x \right) q_k(t) \\ &= \int_0^{L_b} \phi_l(x) F_j \delta(t) \delta(x - x_j)\, \mathrm{d}x. \end{aligned} \tag{14}$$

Employing the orthonormal relations in equations (9)–(11), an infinite set of independent differential equations can be obtained:

$$\ddot{q}_k(t) + 2\xi_k \omega_k \dot{q}_k(t) + \omega_k^2 q_k(t) = N_k(t), \quad k = 1, 2, \cdots \tag{15}$$

where

$$N_k(t) = \int_D \phi_l(x) F_j \delta(t) \delta(x - x_j)\, \mathrm{d}x = F_j \delta(t) \phi_k(x_j). \tag{16}$$

The solution of modal coordinates can be derived as

$$q_k(t) = \frac{1}{\omega_{d_k}} \int_0^t N_k(t) \mathrm{e}^{-\xi_k \omega_k (t-\tau)} \sin \omega_{d_k} (t - \tau)\, \mathrm{d}\tau + q_k(0) \cos \omega_{d_k} t + \dot{q}_k(0) \frac{\sin \omega_{d_k} t}{\omega_{d_k}}, \quad k = 1, 2, \ldots \tag{17}$$

where

$$\omega_{d_k} = \omega_k \sqrt{1 - \xi_k^2}. \tag{18}$$

$q_k(0)$ and $\dot{q}_k(0)$ are the initial displacement and the initial velocity, respectively. For zero initial conditions, equation (17) is simplified to

$$q_k(t) = \frac{F_j \phi_k(x_j)}{\omega_{d_k}} e^{-\xi_k \omega_k t} \sin \omega_{d_k} t. \tag{19}$$

The displacement response at $x = x_i$ for the beam subject to the impact force acting at $x = x_j$ can be derived as

$$w(x_i, t) = w_i(t) = \sum_{k=1}^{\infty} \phi_k(x_i) q_k(t) = \sum_{k=1}^{\infty} \frac{\phi_k(x_i)\phi_k(x_j) F_j}{\omega_{d_k}} e^{-\xi_k \omega_k t} \sin \omega_{d_k} t$$

$$= \sum_{k=1}^{\infty} \frac{\phi_{k,i}\phi_{k,j} F_j}{\omega_{d_k}} e^{-\xi_k \omega_k t} \sin \omega_{d_k} t \tag{20}$$

where $\phi_{k,i} = \phi_k(x_i)$, $\phi_{k,j} = \phi(x_j)$. The beam acceleration response can be obtained by differentiating the above equation with respect to time twice as follows:

$$a(x_i, t) = a_i(t) = \sum_{k=1}^{\infty} \frac{\phi_{k,i}\phi_{k,j} F_j}{\omega_{d_k}} e^{-\xi_k \omega_k t} \left[(2\xi_k^2 \omega_k^2 - \omega_k^2) \sin \omega_{d_k} t - 2\xi_k \omega_k \omega_{d_k} \cos \omega_{d_k} t \right]. \tag{21}$$

Performing Fourier transform on the above equation, one can get the acceleration frequency response at $x = x_i$:

$$A_{x_i}(\omega) = A_i(\omega) = \sum_{k=1}^{\infty} \frac{\phi_{k,i}\phi_{k,j} F_j}{(\omega_k^2 - \omega^2) + i(2\xi_k \omega_k \omega)} (-\omega_k^2 - i2\xi_k \omega_k \omega). \tag{22}$$

3. IMPACT FORCE PREDICTION FORMULATION

3.1. TIME DOMAIN METHOD

Consider the proportionally damped simply supported beam subject to an unknown impact force at $x = x_j$ as shown in Fig. 1. Assume that the beam acceleration response at $x = x_i$ can be experimentally measured and denoted as $\hat{a}_i(t)$. The theoretically estimated acceleration response can be derived as shown in equation (21) and denoted as $a_i(t)$. In order to formulate the force prediction algorithm, the optimisation problem can be defined as follows:

Objective function:

$$Q_i = \sum_{r=1}^{N_t} [a_i(t_r) - \hat{a}_i(t_r)]^2$$

$$= \sum_{r=1}^{N_t} \left[\sum_{k=1}^{n} \left(\frac{\phi_{k,i}\phi_{k,j} F_j}{\omega_{d_k}} e^{-\xi_k \omega_k t_r} \left[(2\xi_k^2 \omega_k^2 - \omega_k^2) \sin \omega_{d_k} t_r - 2\xi_k \omega_k \omega_{d_k} \cos \omega_{d_k} t_r \right] \right) - \hat{a}_i(t_r) \right]^2. \tag{23}$$

Design variables:

$$F_j, \phi_{k,j}, k = 1, 2, \ldots, n. \tag{24}$$

The objective of the optimisation problem is to minimise the square errors between the estimated and measured acceleration response. A total number of N_t time points are

considered. After the resolution of the optimisation problem, the unknown parameters, F_j and $\phi_{k,j}$ can be determined. Therefore, the amplitude of the impact force is predicted. In particular, $\phi_{k,j}$ that is the jth component of the kth mode shape vector can be expressed as follows:

$$\{D\}_j = \begin{bmatrix} \phi_{1,j} & \phi_{2,j} & \cdots & \phi_{n,j} \end{bmatrix}^T. \tag{25}$$

$\{D\}_j$ is the vector containing the jth components of all mode shape vectors at location x_j. The modal matrix of the structure can be expressed as follows:

$$[\Phi] = \begin{bmatrix} \{\phi\}_1 & \{\phi\}_2 & \cdots & \{\phi\}_n \end{bmatrix} = \begin{bmatrix} \phi_{1,1} & \phi_{2,1} & \cdots & \phi_{n,1} \\ \phi_{1,2} & \phi_{2,2} & \cdots & \phi_{n,2} \\ \vdots & \vdots & \ddots & \vdots \\ \phi_{1,m} & \phi_{2,m} & \cdots & \phi_{n,m} \end{bmatrix} = \begin{bmatrix} [G]_1 \\ [G]_2 \\ \vdots \\ [G]_m \end{bmatrix} \tag{26}$$

where

$$[G]_l = \begin{bmatrix} \phi_{1,l} & \phi_{2,l} & \cdots & \phi_{n,l} \end{bmatrix} = \{\hat{D}\}_l^T, \; l = 1, 2, \ldots, n. \tag{27}$$

n is the number of modes, and m is the number of divisions in structures.

Modal assurance criterion (MAC) [18] is usually used to evaluate the correlation between the theoretical and experimental mode shape vectors. Here, MAC_{jl} is used to determine the correlation between $\{D\}_j$ and $\{\hat{D}\}_l$ and defined as follows:

$$MAC_{jl} = MAC\left(\{D\}_j, \{\hat{D}\}_l\right) = \frac{\left|\{D\}_j^T \{\hat{D}\}_l^T\right|^2}{\left(\{D\}_j^T \{D\}_j^*\right)\left(\{\hat{D}\}_l^T \{\hat{D}\}_l^*\right)}, \quad l = 1, 2 \cdots, n. \tag{28}$$

When MAC_{jl} is equal or close to 1, both $\{D\}_j$ and $\{\hat{D}\}_l$ have very good correlation. It is noted that $\{\hat{D}\}_l$ is a row of modal matrix as defined in equation (27) and considered to be known. The modal matrix is one of the structural modal parameters and can be obtained through experimental modal testing or from theoretical modal analysis. When MAC_{jl} equals or is close to 1, $\{D\}_j$ and $\{\hat{D}\}_l$ are well correlated. The impact force location can then be predicted for $j = l$, i.e. $x_j = x_l$.

3.2. FREQUENCY DOMAIN METHOD

Let $A_i(\omega)$ and $\hat{A}_i(\omega)$ denote the theoretically estimated and experimentally measured acceleration frequency response of the beam, respectively. $A_i(\omega)$ has been derived as shown in equation (22). Similar to the time domain method, the optimisation problem can be defined as follows:

Objective function:

$$Q_\omega = \sum_{r=1}^{N_\omega} \left[A_i(\omega_r) - \hat{A}_i(\omega_r)\right]^2$$

$$= \sum_{r=1}^{N_\omega} \left[\sum_{k=1}^{n} \left(\frac{\phi_{k,i}\phi_{k,j}F_j}{(\omega_k^2 - \omega_r^2) + i(2\xi_k\omega_k\omega_r)} \left(-\omega_k^2 - i2\xi_k\omega_k\omega_r\right) \right) - \hat{A}_i(\omega_r) \right]^2 \tag{29}$$

Design variables:

$$F_j, \; \phi_{k,j}, \; k = 1, 2, \ldots. \tag{30}$$

The objective is to minimise the square errors between the estimated and measured acceleration frequency response. A total number of N_ω frequency points are considered. F_j and $\phi_{k,j}$ can be determined by the resolution of the optimisation problem. Therefore, the amplitude of the impact force is predicted. Through the evaluation of MAC_{jl} as shown in equation (28), the impact force location can also be predicted.

4. IMPLEMENTATION OF PREDICTION MODEL

The force prediction program is implemented with MS-FORTRAN Power Station. Visual Numerics IMSL Math Library is adopted to solve the optimisation problem [19]. The program flowchart is shown in Fig. 2 and briefly summarized as follows:

1. Set up the initial guesses of design variables. The initial values of the impact force amplitude F_j and mode shape information $\phi_{k,j}, k = 1, 2, \ldots, n$ are specified. In this work, $n = 4$ is adopted, i.e. four modes are included to construct the structural response.

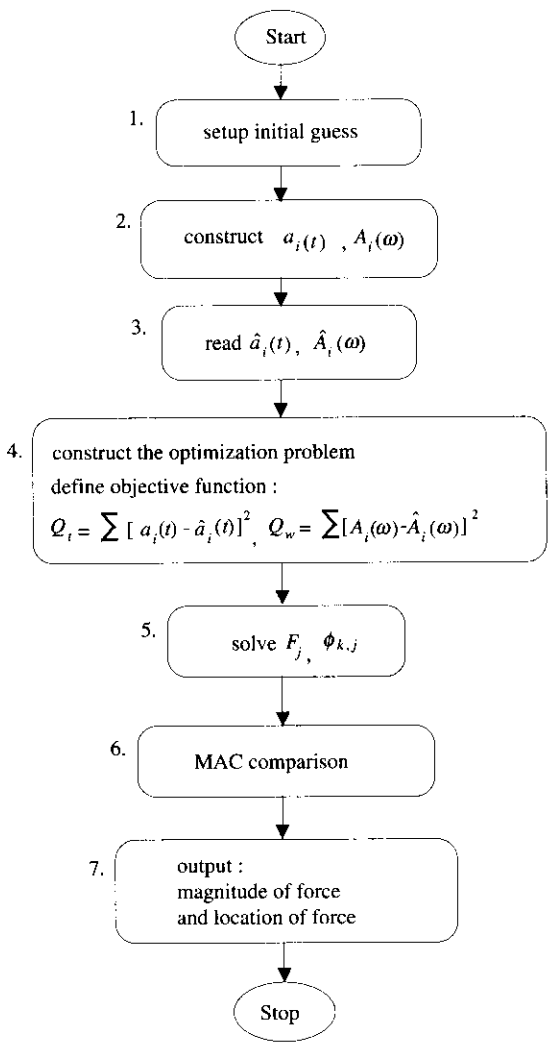

Figure 2. Program flow chart.

TABLE 1

Three options in evaluating the objective functions

Option	Response	
	$a_i(t)$ or $A_i(\omega)$	$\hat{a}_i(t)$ or $\hat{A}_i(\omega)$
Option I	Use theoretical modal parameters to estimate the response $a_i(t)$ or $A_i(\omega)$	Use theoretical response $a_i(t)$ or $A_i(\omega)$ to represent $\hat{a}_i(t)$ or $\hat{A}_i(\omega)$
Option II	Use theoretical modal parameters to estimate the response $a_i(t)$ or $A_i(\omega)$	Use experimentally measured response $\hat{a}_i(t)$ or $\hat{A}_i(\omega)$
Option III	Use experimentally extracted modal parameters to estimate $a_i(t)$ or $A_i(\omega)$	Use experimentally measured response $\hat{a}_i(t)$ or $\hat{A}_i(\omega)$

2. Construct the predicted response $a_i(t)$ or $A_i(\omega)$. Equation (21) or (22) is applied to estimate the beam acceleration response in the time or frequency domain, respectively.
3. Read experimentally measured response $\hat{a}_i(t)$ or $\hat{A}_i(\omega)$. The accelerometer is applied at the known location $x = x_i$. The acceleration response due to the unknown impact force is measured and input to the prediction program.
4. Construct the optimisation problem. The objective functions as shown in equations (23) and (29) for both the time and frequency domain methods can be formulated and expressed as functions of the force amplitude and location associated with mode shape components.
5. Solve the optimisation problem. The impact force amplitude F_j and mode shape information $\phi_{k,j}, k = 1, 2, \ldots, n$ can be determined.
6. Compare MAC_{jl}. From equation (28), the impact force location can also be predicted.
7. Print out prediction results.

The program has three options based on the selection of theoretical response of $a_i(t)$ or $A_i(\omega)$ and the experimental response of $\hat{a}_i(t)$ or $\hat{A}_i(\omega)$. Both the estimated response and measured response in the objective functions shown in equations (23) and (29) for the optimisation problems are needed in order to predict the impact force amplitude and location. The three options are tabulated in Table 1. The purpose and their applications of the three kinds of combinations are explained as follows:

Option I: Use theoretical modal parameters to estimate $a_i(t)$ or $A_i(\omega)$ incorporated with the theoretical response to represent $\hat{a}_i(t)$ or $\hat{A}_i(\omega)$ instead of experimentally measured ones. This approach is simply a numerical simulation and mainly for the validation of the developed force prediction methods.

Option II: Use theoretical modal parameters to estimate $a_i(t)$ or $A_i(\omega)$ incorporated with the experimentally measured response $\hat{a}_i(t)$ or $\hat{A}_i(\omega)$. The idea of this approach can be applied to complex structures that are not easy or feasible to experimentally determine the modal parameters of the structure. The modal parameters used in equations (23) and (29) are derived from theoretical modal analysis.

Option III: Use the experimentally extracted modal parameters to estimate response $a_i(t)$ or $A_i(\omega)$ incorporated with the experimentally measured response $\hat{a}_i(t)$ or $\hat{A}_i(\omega)$. This option is suitable for the case where the experimental modal parameters can be extracted experimentally or where the theoretical modal analysis of structures is not possible.

5. RESULTS AND DISCUSSIONS

This section presents the force prediction results for the simply supported beam subject to an unknown impact force. The impact hammer (BK8202) implements the unknown

TABLE 2

Physical properties of simply supported beam

Material	Steel
Length	0.38 m
Width	0.04 m
Thickness	0.002 m
Density	7870 kg/m^3
Young's modulus	207×10^9 N/m^2
Poisson ratio	0.292

impact force. The force signal can be recorded for the comparison with the predicted results. Both numerical simulation and experimental verification are carried out to demonstrate the feasibility of the developed force prediction algorithm. The physical properties of the simply supported beam are shown in Table 2. The simply supported beam had been experimentally and successfully validated for its structural modal parameters [20]. The simply supported beam is divided into 19 divisions and numbered as shown in Fig. 1. The developed force prediction models for both time and frequency domain methods are applied to determine the impact force amplitude and location.

5.1. THEORETICAL MODAL PARAMETERS WITH THEORETICAL RESPONSE (OPTION 1)

Table 3(a) shows the prediction of the impact force amplitude for different force locations at division points. Symbol (i, j) denotes the measurement point at position i and the impact force applied at position j. In Table 3(a), four cases are presented. The accelerometer is located at position 1 to measure the acceleration response, the impact force is applied at positions 5, 7, 10 and 18, respectively. One can observe that the amplitudes of the impact force for both time and frequency domain methods are reasonably predicted.

Figure 3(a) and 3(b) shows the predicted force locations corresponding to the cases in Table 3(a) for both time and frequency domain methods, respectively. The horizontal axis is the position number of the beam from 1 to 19 as shown in Fig. 1. The vertical axis is the MAC values as defined in equation (27). The actual impact force location is also depicted as shown by the arrows. As discussed previously, when MAC value equals or is close to 1, the corresponding number of position will be the impact force location. One can observe that for frequency domain method as shown in Fig. 3(b), the location prediction is very good. For the time domain method, the location prediction is also good except in case of $j = 10$. This can be the reason why position $j = 10$ is right on the nodal point of even modes. However, the MAC value is relatively larger at position 10 than elsewhere.

Table 3(b) shows the prediction of the impact force amplitude for different force locations at non-division points, i.e. $(i,j) = (3,18.5)$ and $(i,j) = (10,2.5)$. $j = 18.5$ means that the impact force is applied at the middle between positions 18 and 19. The predicted amplitudes reveal a relatively larger difference than those cases of force applied at division points. This discrepancy may come from the nature of the prediction algorithm that is based on the resolution of division points. Figure 4 shows the predicted location for the two cases. As seen from Fig. 4, both the time and frequency domain methods provide quite good prediction except in the case of $(i,j) = (10,2.5)$ for the time domain method. It is

TABLE 3

Prediction of force amplitude for different force locations (Option I)

(a) *At division points*	F_j(N)		
(i,j)	Actual value	Predicted value (time method)	Predicted value (freq. method)
(1,5)	1.000	0.762	0.763
(1,7)	1.500	1.504	1.058
(1,10)	0.800	0.734	1.253
(1,18)	0.799	0.850	0.976
(b) At non-division points			
(3,18.5)	0.380	0.194	0.261
(10,2.5)	0.537	1.575	0.560

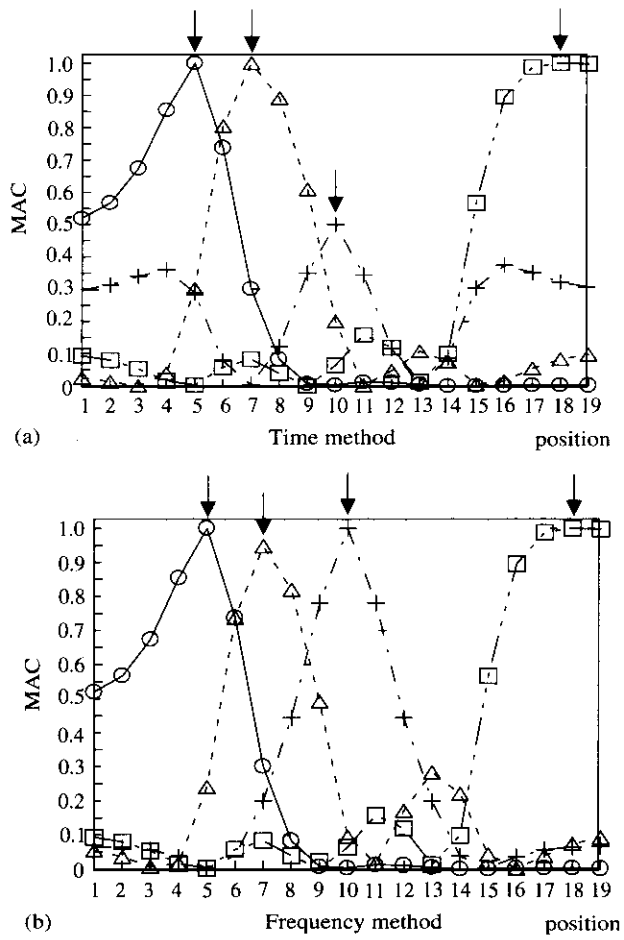

Figure 3. Prediction of force location for different force locations at division points (Option I). (a) Time domain method; (b) frequency domain method: -⊖-, J position at 5; - △ -, J position at 7; —+ -, J position at 10; —□—, J position at 18.

noted that MAC values at the force position for the two cases are near 0.9 that is close to 1 but not perfectly 1. It is a fact that the force locations are at the non-division points. Nevertheless, the algorithm predicts the trend of the force location.

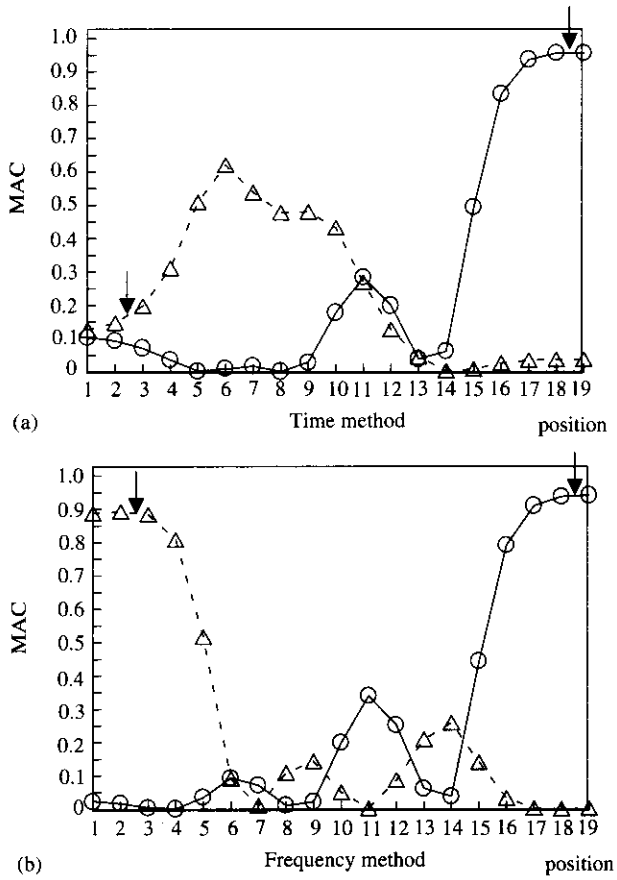

Figure 4. Prediction of force location for different force locations at non-division points (Option I). (a) Time domain method; (b) Frequency domain method: —⊖—, J position at 18.5; · △ ·, J position at 2.5.

TABLE 4

Prediction of force amplitude for different force amplitudes (Option I)

(i, j)	F_j(N)		
	Actual value	Predicted value (time method)	Predicted value (freq. method)
(3,2)	1.470	0.942	1.201
(3,2)	0.581	0.579	0.581
(1,18)	0.350	0.280	0.669
(1,18)	0.799	0.850	0.976

For the impact forces acting at the same location, i.e. $j=2$ or 18, but different force amplitudes, Table 4 shows that both the time and frequency domain methods provide satisfactory prediction of force amplitudes. Although the predicted force amplitudes are somewhat different from the actual values, the prediction for the variation of force amplitude is quite consistent.

It is also interesting to study the effect of different accelerometer locations on the force prediction. Let the impact force be applied at position 18, and the accelerometers be

TABLE 5

Prediction of force amplitude for different measurement points (Option I)

	F_j(N)		
(i, j)	Actual value	Predicted value (time method)	Predicted value (freq. method)
(1,18)	0.799	0.850	0.976
(5,18)	0.883	0.598	1.099
(7,18)	0.560	0.399	1.119
(10,18)	1.110	0.728	1.561

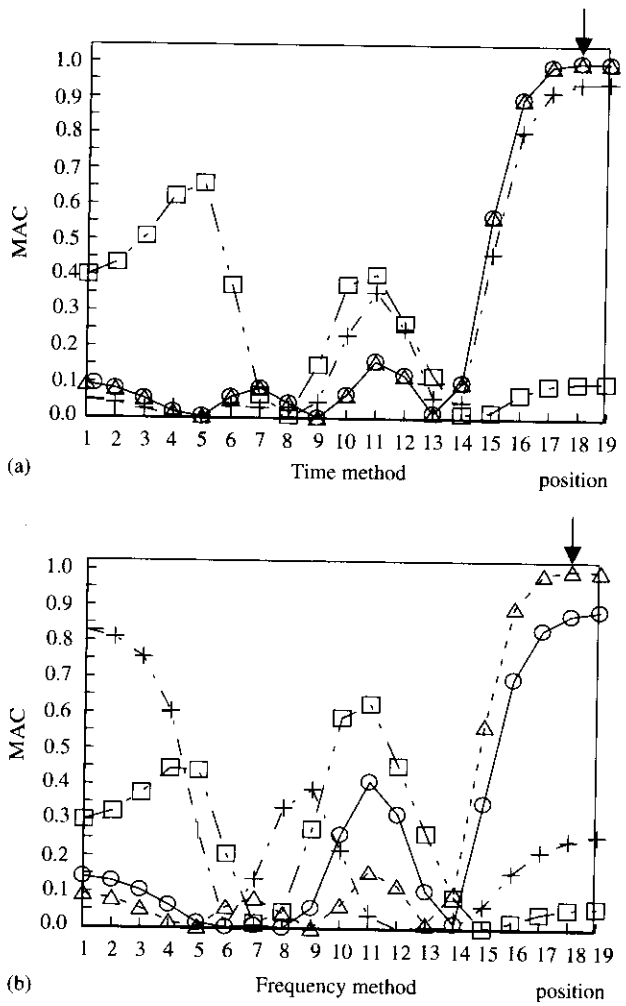

Figure 5. Prediction of force location for different measurement points (Option I). (a) Time domain method; (b) Frequency domain method: · ⊖—, I position at 1; - △ -, I position at 5; —|- -, I position at 7; —⊟—, I position at 10.

located at positions 1, 5, 7 and 10, respectively. Table 5 shows that the prediction of force amplitude is acceptable, although the results from the frequency domain method are slightly overestimated. Figure 5 shows the prediction of force locations corresponding to

the cases of Table 5. Most of the cases reveal very good location prediction except for the case of measurement point at $i = 10$. The position 10 is right at the middle of the beam as known to be the nodal points of even modes. It is reasonable to conclude that the measurement points should be better located away from nodal points.

5.2. THEORETICAL MODAL PARAMETERS WITH EXPERIMENTAL RESPONSE (OPTION II)

As discussed, Option II is to use theoretical modal parameters to estimate the system response, while the experimentally measured response is actually used. Table 6 shows the prediction of force amplitudes for different force locations. The prediction is not quite good, but some predictions are near the actual force amplitude. The discrepancy may be due to the fact that the actual impact force is triangle shaped in time domain as shown in Fig. 6. However, in this work the impact force is simulated by an ideal impulsive force function. The assumption of the idealised impact force will cause the predicted amplitude to be relatively smaller than the actual ones.

Figure 7 shows the prediction of force location corresponding to the cases of Table 6. One can see that the location prediction is reasonably good except for the case in which the force is applied at position 19. This can be the reason why the measurement point is at

TABLE 6

Prediction of force amplitude for different force locations (Option II)

	F_j(N)		
(i, j)	Actual value	Predicted value (time method)	Predicted value (freq. method)
(3,2)	0.581	0.500	0.144
(3,19)	1.600	1.478	0.027
(3,18.5)	0.380	0.675×10^{-6}	0.173
(10,2.5)	0.537	0.142	0.126

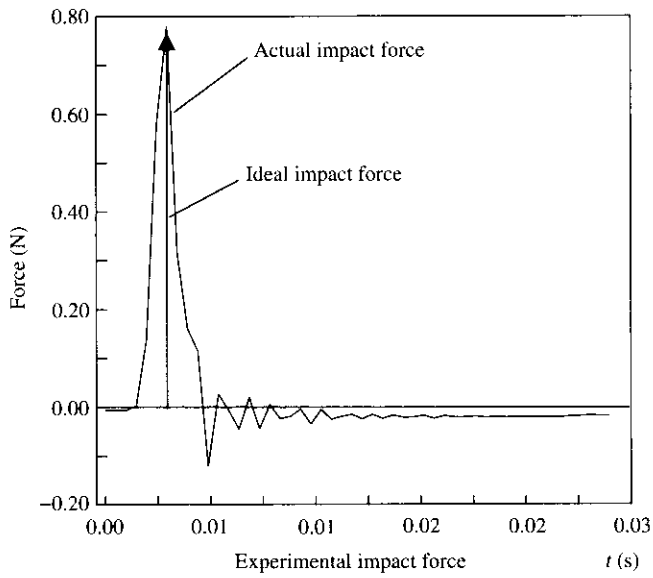

Figure 6. Typical time history of actual impact force.

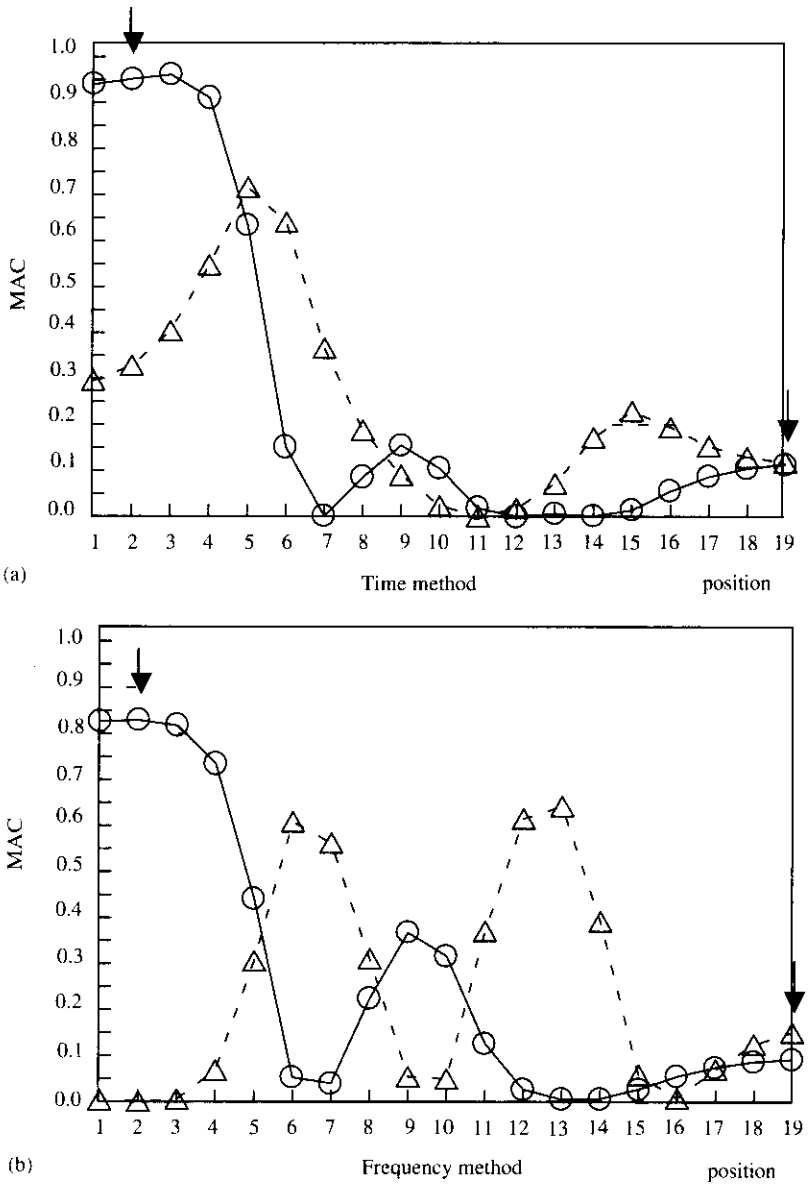

Figure 7. Prediction of force location for different force locations (Option II). (a) Time domain method (division point); (b) frequency domain method (division point): ○ , J position at 2; △ , J position at 19. (c) Time domain method (non-division point); (d) frequency domain method (non-division point): —⊖—, J position at 18.5; ⩚ , J position at 2.5.

position 3 away from the force location [9]. Another reason may be that the assumption of an ideal impulsive force is not appropriate and needs to be revised to the triangular force instead of the unit impulse force.

For the cases of different force amplitudes, Table 7 shows that both time and frequency domain methods can predict the variation of force amplitude, but the exact amplitude value is generally underestimated. As mentioned previously, this may be due to the

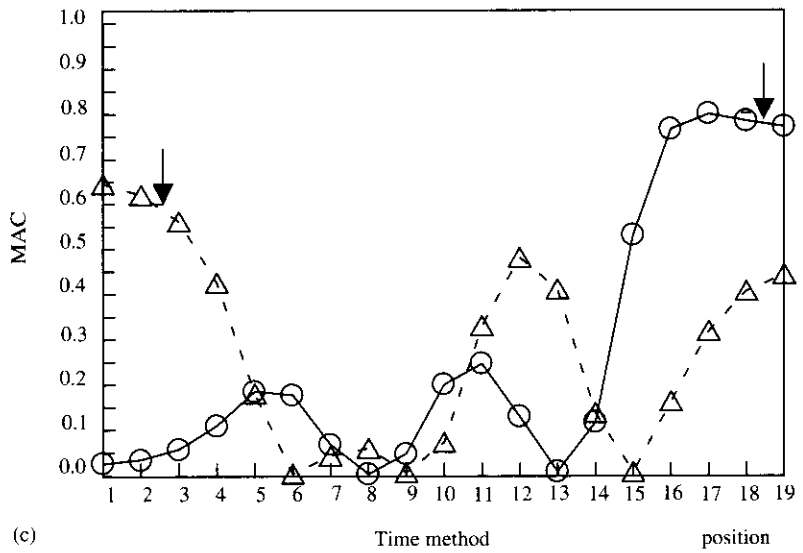

(c)

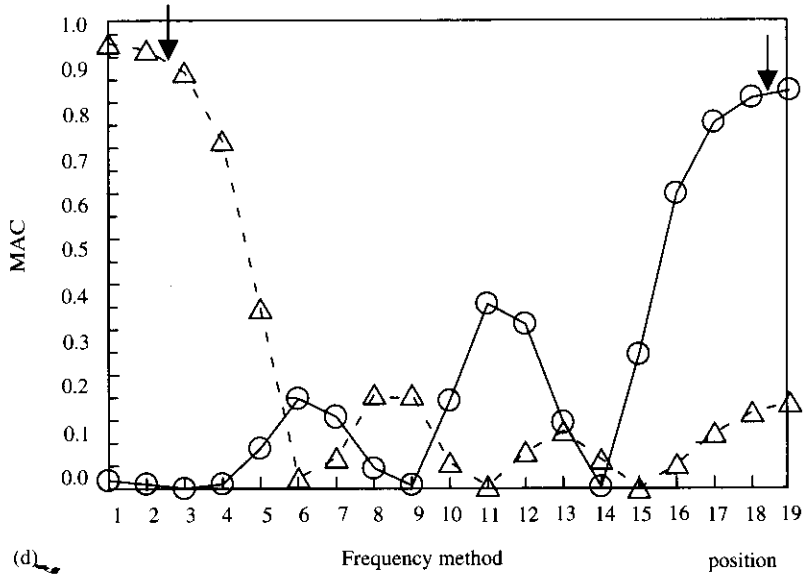

(d)

Figure 7. (Continued.)

TABLE 7

Prediction of force amplitude for different force amplitudes (Option II)

	F_j(N)		
(i, j)	Actual value	Predicted value (time method)	Predicted value (freq. method)
(3,2)	1.470	0.301	0.093
(3,2)	0.581	0.500	0.144
(1,18)	0.350	0.349	0.244×10^{-3}
(1,18)	0.799	0.449	0.0134

TABLE 8

Prediction of force amplitude for different measurement points (Option II)

	F_j(N)		
(i, j)	Actual value	Predicted value (time method)	Predicted value (freq. method)
(1,18)	0.799	0.449	0.0134
(5,18)	0.883	0.016	0.048
(7,18)	0.560	0.004	0.316
(10,18)	1.110	0.343×10^{-4}	0.306

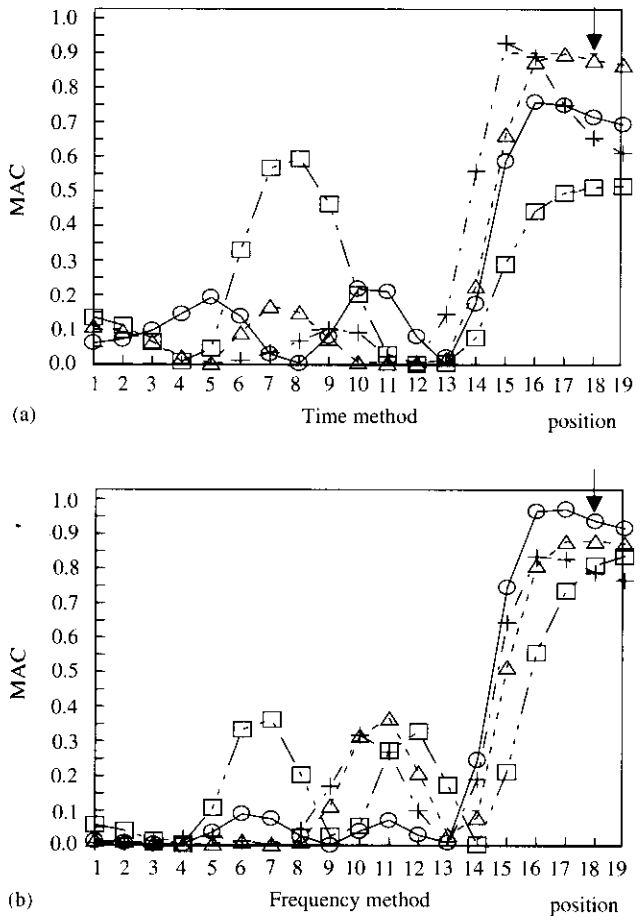

Figure 8. Prediction of force location for different measurement points (Option II). (a) Time domain method; (b) frequency domain method: —○—, I position at 1; · △ ·, I position at 5; —+—, I position at 7; —□—, I position at 10.

improper assumption of ideal impact force. The modification of the impact force to a triangular force may improve the prediction algorithm.

To discuss the effect of measurement points on the prediction model, let the impact force be fixed at position 18. Table 8 shows that the predictive force amplitudes are generally smaller than the actual values. Corresponding to the cases of Table 7, Fig. 8 shows that the force location can generally be well predicted. In summary, the

prediction algorithm is again shown for its feasibility, especially, in determining the force location.

5.3. EXPERIMENTAL MODAL PARAMETERS WITH EXPERIMENTAL RESPONSE (OPTION III)

In this section, the impact force prediction for Option III is presented. The force location is also considered for acting at both division and non-division points. Table 9 shows that the predictive force amplitudes are generally smaller than the actual values. This again can be due to the improper assumption of the unit impulsive force. Figure 9, corresponding to the cases of Table 8, reveals that the force acting at position 2 can be reasonably predicted, and the force acting at position 19 can only be predicted for its possibility because to the measurement point is at position 3 far away from the force location. The force amplitude may not have good prediction due to the improper assumption for modelling the impact force. The location of force can be generally predicted, if the measurement points can be properly selected.

Table 10 shows the results for the prediction of different force amplitudes. The prediction is not good enough for force variation and it also does not approach the actual value. It is necessary to modify the assumption of the impact force for estimating the response so as to improve the algorithm and is under investigation.

Figure 10 shows the prediction of force location for different measurement points, while the impact force is applied at position 18. Except for the case of measurement point at position 10 which is not good, the other cases provide a satisfactory prediction of force location. However, some false predicted locations may occur. Table 11 shows the prediction of force amplitudes that are generally smaller than the actual values as discussed previously. For the present study, the impact force is modelled by an ideal impulsive delta function. The prediction of force amplitudes for practical applications may be underestimated, while the developed predictive models can provide a reasonable prediction of force location. The new approach shows its potential in predicting the impact force amplitude and location simultaneously. The modelling modification for the ideal impact force to a triangular force as shown in Fig. 6 will help to improve the prediction results, in particular, for the force amplitude and is under investigation.

6. CONCLUSIONS AND RECOMMENDATIONS

This work develops a new approach for the impact force prediction methods to determine the force amplitude and location of an unknown impact force simultaneously. With the prior knowledge of structural information in terms of modal parameters, when the accelerometer is applied to measure the structural response due to the impact force, the

TABLE 9

Prediction of force amplitude for different force amplitudes (Option III)

	F_j(N)		
(i, j)	Actual value	Predicted value (time method)	Predicted value (freq. method)
(3,2)	0.581	0.093	0.089
(3,19)	1.600	0.022	0.138×10^{-4}
(3,18.5)	0.380	0.170×10^{-3}	0.860×10^{-3}
(10,2.5)	0.537	0.468×10^{-5}	0.054

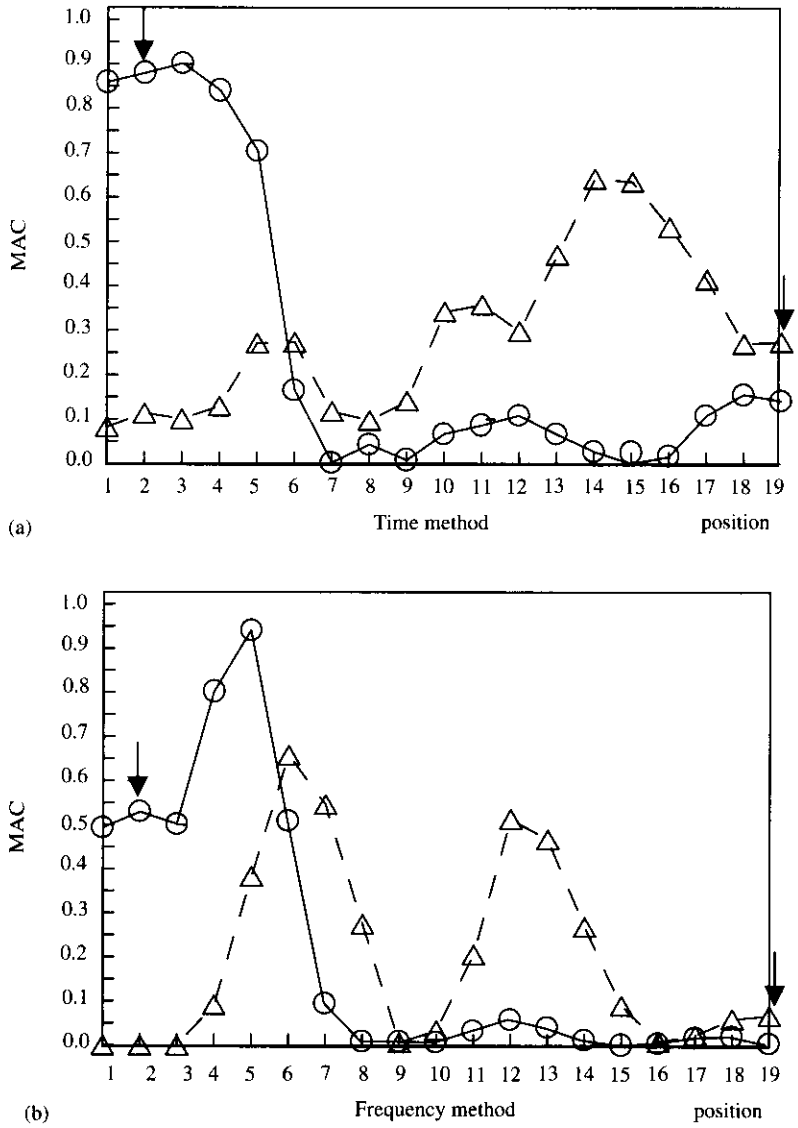

Figure 9. Prediction of force location for different force locations (Option III). (a) Time domain method (division point); (b) frequency domain method (division point): —⊖—, J position at 2; - △ -, J position at 19. (c) Time domain method (non-division point); (d) frequency domain method (non-division point): —⊖—, J position at 18.5; - △ -, J position 2.5.

force magnitude and location can be determined by the solution of formulated optimisation problem. The ideal impulse force is assumed to model the actual impact force. Both time and frequency domain methods are presented. The force prediction models are numerically and experimentally demonstrated. Some conclusions are summarised as follows:

1. The predictive model considers using theoretical modal parameters to estimate the response incorporated with the theoretical response (Option I) to demonstrate the

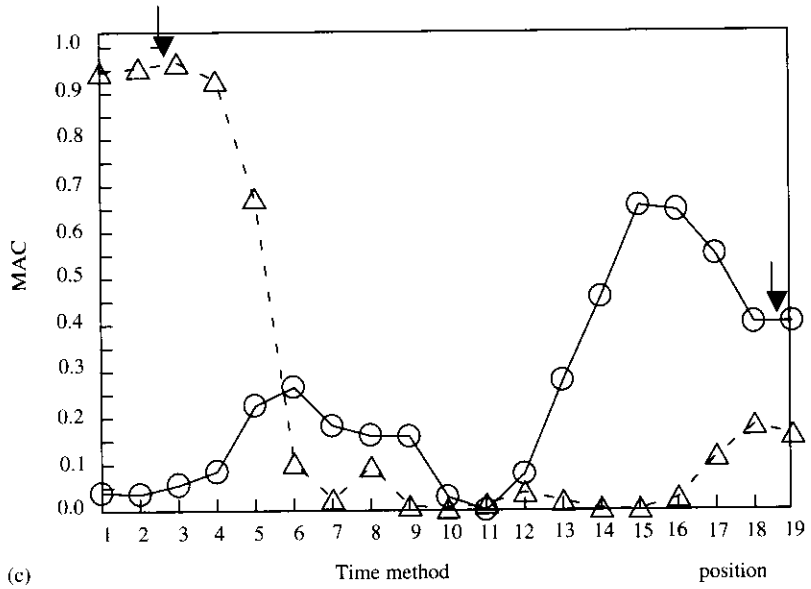

(c)

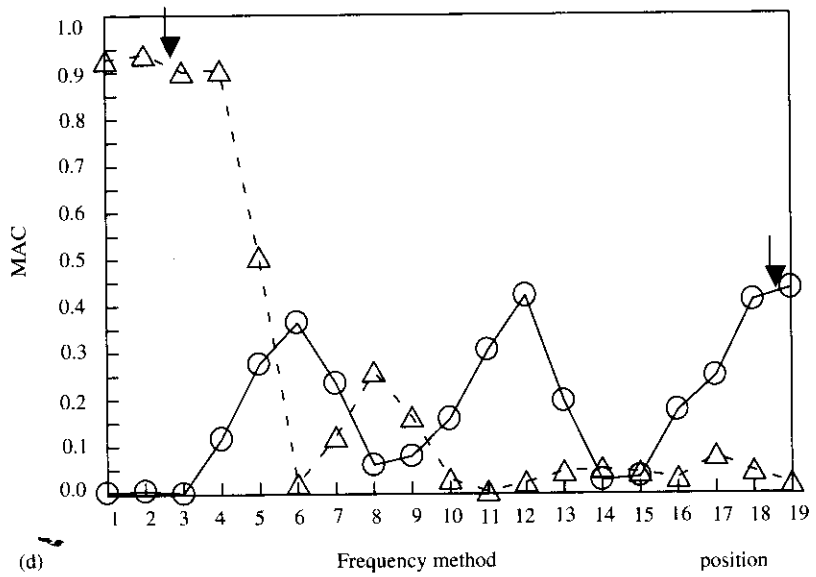

(d)

Figure 9. (continued).

feasibility of the developed algorithm. Results show that the predictive model can determine the location and amplitude satisfactorily. The effects of different force amplitudes and locations as well as different measurement locations on the prediction are also studied.

2. When structural modal parameters are not available, the estimated response by using the theoretical modal parameters can be incorporated with the experimental response (Option II) to determine the impact force amplitude and location.
3. If both the system modal parameters and system response can be determined from experiments, Option III approach can be adopted and is also shown for the potentials of the developed predictive model.

TABLE 10

Prediction of force amplitude for different force amplitudes (Option III)

	F_j(N)		
(i, j)	Actual value	Predicted value (time method)	Predicted value (freq. method)
(3,2)	1.470	0.147	0.123
(3,2)	0.581	0.093	0.089
(1,18)	0.350	0.370×10^{-2}	0.011
(1,18)	0.799	0.260	0.001

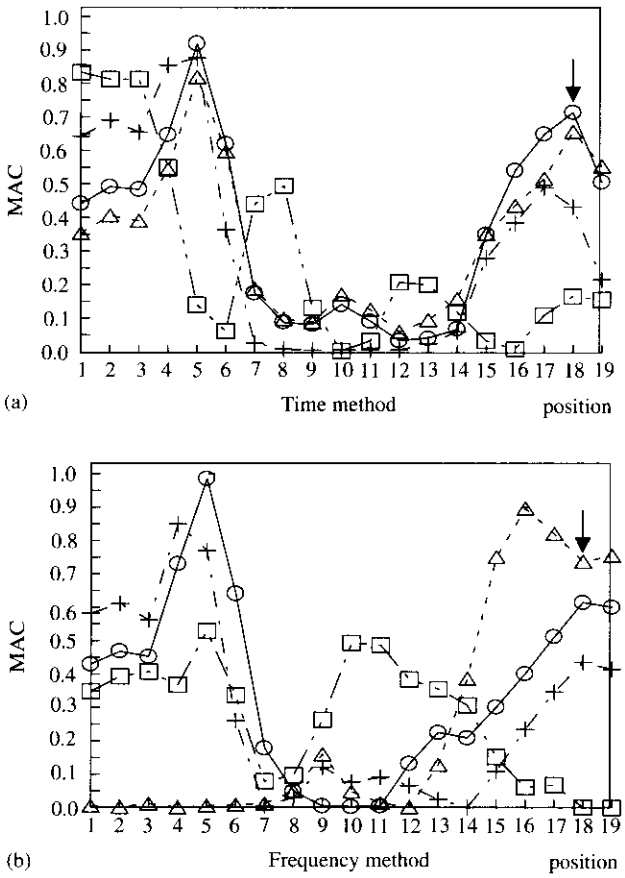

Figure 10. Prediction of force location for different measurement points (Option III). (a) Time domain method; (b) frequency domain method: -○-, 1 position at 1; -△-, 1 position at 5; -+-, 1 position at 7; -□-, 1 position at 10.

4. The developed force predictive algorithm has better adaptation in determining the force location than the force amplitude.
5. The actual impact force has a triangular shape in time domain. The modification of impact force function to a triangular form may be required for better force amplitude prediction and is under investigation.

TABLE 11

Prediction of force amplitude for different measurement points (Option III)

	F_j(N)		
(i, j)	Actual value	Predicted value (time method)	Predicted value (freq. method)
(1,18)	0.799	0.260	0.001
(5,18)	0.883	0.031	0.150×10^{-4}
(7,18)	0.560	0.203	0.029
(10,18)	1.110	0.092	0.143

ACKNOWLEDGEMENTS

The authors profusely thank the partial supports for this work from National Science Council of Republic of China under the contract number NSC88-2212-E-020-001.

REFERENCES

1. K. K. STEVENS 1987 *Proceeding of the 1987 SEM Conference on Experimental Mechanics* June, 838–844. Force identification problems—an overview, Houston, TX.
2. M. C. HAN and A. L. WICKS 1990 *Proceedings of the 8th International Modal Analysis Conference,* 365-372. Force determination with slope and strain response measurement, Kissimmee, FL.
3. H. INOUE, N. IKEDA, K. KISHIMOTO, T. SHIBUYA and T. KOIZUMI 1995 *JSME International Journal Series A* **38**, 84–91. Inverse analysis of the magnitude and direction of impact force.
4. T. W. LIM and W. D. PILKEY 1992 *Computer and Structures* **43**, 53–59. A solution to the inverse dynamics problem for lightly damped flexible structure using a modal approach.
5. H. R. BUSBY and D. M. TRUJILLO 1987 *Computer and Structures* **25**, 109–117. Solution of an inverse dynamics problem using an eigenvalue reduction technique.
6. J. ZHU and Z. LU 1991 *Journal of Sound and Vibration* **148**, 137–146. A time domain method for identifying dynamic loads on continuos system.
7. E. WU, J. C. YEH and C. S. YEN 1994 *International Journal of Impact Engineering* **15**, 417–433. Impact on composite laminated plates: an inverse method.
8. C. CHANG and C. T. SUN 1989 *Experimental Mechanics* **29**, 414–419. Determining transverse impact force on a composite laminate by signal deconvolution.
9. P. E. HOLLANDSWORTH and H. R. BUSBY 1989 *International Journal of Impact Engineering* **8**, 315–322. Impact force identification using the general inverse technique.
10. S. ODEEN and B. LUNDBERG 1991 *International Journal of Impact Engineering* **11**, 149–158. Prediction of impact force by impulse response method.
11. D. M. LIU, C. Z. TSAI and E. WU 1997 *Proceedings of 14th national Conference of the Chinese Society of Mechanical Engineers*, 347–354. A new non-contact technique to identify impact force of beam structure (in Chinese), Taoguan, Taiwan.
12. E. WU, J. C. YEN and C. S. YEN 1994 *AIAA Journal* **34**, 2433–2439. Identification of impact forces at multiple locations on laminated plates.
13. J. F. DOYLE 1987 *Experimental Mechanics* **27**, 229–233. An experimental method for determining the location and time of initiation of an unknown dispersing pulse.
14. J. F. DOYLE 1994 *Experimental Mechanics* **34**, 37–44. A genetic algorithm for determining the location of structural impact.
15. M. T. MARTIN and J. F. DOYLE 1996 *International Journal of Impact Engineering* **18**, 79–97. Impact force location in frame structures.
16. K. CHOI and F. K. CHANG 1996 *AIAA Journal* **34**, 136–142. Identification of impact force and location using distributed sensors.
17. L. MEIROVITCH 1967 *Analytical Methods in Vibrations*. London, UK: The MacMillan Company.

18. D. J. EWINS 1995 *Modal Testing: Theory and Practice*. Taunton, Somerset, UK, Research Studies Press Ltd.
19. IMSL, Inc. 1989 *MATH/LIBRARY FORTRAN Subroutines for Mathematical Applications*, Houston, TX.
20. C. H. CHIU, B. T. WANG and D. H. WU 1998 *Proceedings of the 15th National Conference of Chinese Society of Mechanical Engineering*, 291–298. The validation of modal properties for simply supported beam (in Chinese) Tainai, Taiwan.